INTEGRATING TENSILE PARAMETERS IN 3D MASS-SPRING SYSTEM

V. BAUDET[1,2], M. BEUVE[2], F. JAILLET[2], B. SHARIAT[2], F. ZARA[2]

(1) LSIIT-IGG, UMR CNRS 7005, Illkirch, F-67412, France
E-mail: vincent.baudet@gmail.com
(2) LIRIS-SAARA, UMR CNRS 5205, Université Lyon 1,Villeurbanne, F-69622, France
E-mail: {mbeuve,fjaillet,bshariat,fzara}@liris.cnrs.fr

1. INTRODUCTION

In Computer Graphics, deformable object animation by physically based models is often achieved by use of mass-spring system. Indeed, such discrete model makes it possible to obtain interactive animation time, even for complex scene, hardly reach with other more complex models. At the contrary, although visually credible, these mass-spring models do not permit to easily integrate physical properties data, making thus difficult to render physically correct simulations.
For this reason, we propose in this paper a new 3D formulation achieved by assembling elemental bricks made up of vertices and edges, which are next transformed into a mass-spring system: vertices or masses, are thus connected along the edges by the mean of springs. Our model strength lies then in the analytic determination of the spring coefficient values (stiffness), making it possible to reproduce the behaviour of any object. Thus, the stiffness values of the discrete model are directly deduced from the mechanical properties of the real object (elasticity, shearing, compressibility, etc.).
We validate our model by handling some experiments like shearing or inflexion. In particular, comparisons are made between our model and a reference solution. This new discrete model could then be useful to interactively simulate the behaviour of soft tissues (whose mechanical parameters are known), for example within the framework of medical simulators.

Keywords: Animation by physical models, Mass-spring system, Elasticity parameters

2 RELATED WORKS

Mass-spring systems have largely been used in the animation context, because of their simple implementation and their possible applications for a large panel of deformations. An important problem of these models is to choose an appropriate

meshing, as springs stiffness constants are generally empirically set [5].
Solution based on optimisation algorithms [2,4] may provide with automated stiffness determination. However, its efficiency depends on the number of springs and requires expensive computation time. Moreover, the process should be repeated after any mesh alteration.
Direct analytic solution to parameterise the springs should save computer resources. The Mass-Tensor approach [3,6] aims at simplifying finite element method theory by discretising the constitutive equations. Despite its interest, this approach requires pre-computations and storage of an extensive amount of information for each mesh component.
Van Gelder has proposed an approach highly referenced [7]. A new formulation is given for triangular meshes, allowing calculating spring stiffness according to elastic parameters. However, numerical simulations completed by a Lagrangian analysis exhibited the incompatibility of the proposal with the physical reality. Therefore, controlling realistically the elastic parameters has been proved difficult [1].

3 TENSILE PROPERTIES AND EXPERIMENTS

Linear elastic isotropic and homogeneous material can be characterized by four parameters: Young's modulus, Poisson's ratio, shear modulus and bulk modulus. They are generally extracted by a set of experiments (Fig. 1).

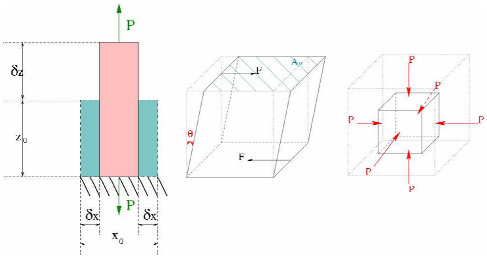

Figure 1: The 3 physical experiments: elongation, shearing, inflation (from left to right).

Elongation experiment
The Young's modulus and the Poisson's ratio are measured by elongation experiments, measuring alterations on each axe as response to a pressure ***P***. The Young's modulus E (in Pa) defines the elasticity of a material by:

$$E = \frac{\left|\vec{P}\right|}{\delta z / z_0}.$$

Poisson's ratio ν (without unit) characterizes the thinning ($2\delta i / i_0$ with $i \in (x, y)$) induced by the elongation:

$$\nu = -\left(\frac{2\delta i}{i_0}\right) / \left(\frac{\delta z}{z_0}\right).$$

Shearing experiment
The deviation angle θ (Fig. 1) is induced by two opposite forces ***F***, and characterises the shearing amplitude G:

$$G = \left(\frac{\left|\vec{F}\right|}{A_0}\right) / (\tan(\theta)) \sim \left(\frac{\left|\vec{F}\right|}{A_0}\right) / \theta \text{ when } \theta \to 0,$$

with A_0, the area of the base. For small deformations, it reads: $G = E/2(1+\nu)$.

Inflation experiment
It consists in measuring the inflation ΔV resulting from a concentric pressure ΔP, applied to each face (Fig. 1). The Bulk modulus B is defined by (* for small deformations):

$$B = (\Delta P) / \left(\frac{\Delta V}{V_0}\right), \quad *B = E/3(1-2\nu).$$

4. OUR 3D MODEL

To be able to reproduce the mechanical behaviour with mass-spring systems, we have to determine the stiffness coefficient of the springs to match real materials. We propose to carry out numerically the experiments previously described, and to establish a relation between the stiffness coefficients and the imposed tensile parameters.

We consider as sample a $x_0 \times y_0 \times z_0$ parallelepiped. Fig. 2 displays the best 3D configuration for these diagonal and edge links. We propose a methodology to calculate these parameters analytically, within the Lagrangian framework. For each experiment on Fig. 1:

(1) We build the Lagrangian as the sum of the springs potential after deformation, as well as the one of external forces (null kinetic term).

(2) We establish a 2nd order Taylor's expansion in deformations and apply least action principle. It reads linear equations.

(3) From section 3, we express the mechanical characteristics according to the stiffness coefficients.

(4) We solve this set of equations (the mechanical characteristics are input parameters).

As it may be noticed, inner diagonals fully define the shearing modulus, thus for a cube, k_d may be determined proportionally to G (and E, ν):

$$k_d = \frac{3Ex_0}{8(1+\nu)}.$$

Next, the non-diagonal edge stiffness k_x (*resp.* k_y, k_z) has to satisfy two relations (E and ν). A solution can be found but restricted to ν=0.25. Thus, we propose to add two new forces $F_\perp$ induced by the elongation. They have to be identical in both directions for symmetry reasons (Fig. 3). It leads to a new system that after resolution reads for $i \in \{x_0, y_0, z_0\}$:

$$k_x = \frac{Ex(4\nu+1)}{8(1+\nu)}, \qquad F_{\perp i} = -\frac{F_i(4\nu-1)}{16}.$$

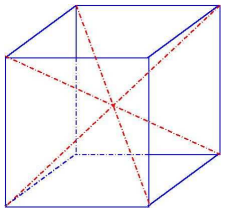

Figure 2: Links in the 3D element

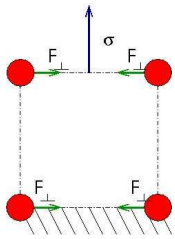

Figure 3: Orthogonal correction forces.

The Lagrangian equation of the inflation test verifies that this solution satisfies the definition of the bulk modulus. Finally, from these parameters, we can tackle the simulation of any object composed of mesh elements:

(1) Compute all forces applied to an element; (i) internal, including forces due to springs and correction forces, or (ii) external, like gravity or interaction with neighbourhood.

(3) Calculate accelerations and velocities according to an integration scheme (explicit or implicit Euler, Verlet, etc.).

(4) Displace each mesh node consequently.

5 EVALUATION OF THE 3D MODEL

As some approximations have been made, effective mechanical properties of our meshed models have been tested against small and large deformations; the more pertinent ones follow.

Limits in shearing

As expected, for a stressed cube, the relative error on G does not depend on E. This error increases with ν, but remains reasonable for small shear angle and compressible material (Fig. 4).

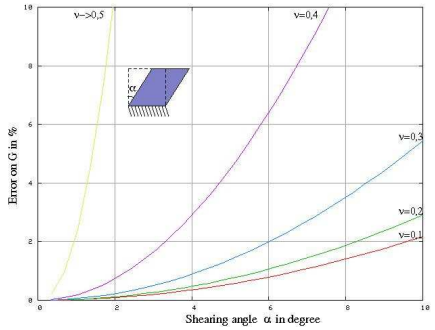

Figure 4: Measured error on shearing in a cube according to E and v

Next, we stress a composite shape. Fig. 5 illustrates the influence of the mesh resolution.

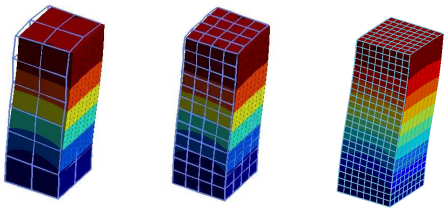

2x2x6 sampling: M=13%, SD=1.3%, MAX=33%
4x4x12 sampling: M=6%, SD=0.33%, MAX=14%
8x8x24 sampling: M=3%, SD=0.03%, MAX=6%

Figure 5: Shearing: superposition of our wired model with a colour gradation FEM reference. (M for Mean Error, SD for Standard Deviation, MAX for Max Error).

Limits in deflection

This experience constitutes a relevant test to evaluate mass repartition and good behaviour in case of large deformations (inducing large rotations).
At equilibrium, under gravity loads, the top of the beam is under tension while the bottom is under compression, leaving the middle line of the beam relatively stress-free (Fig. 6).

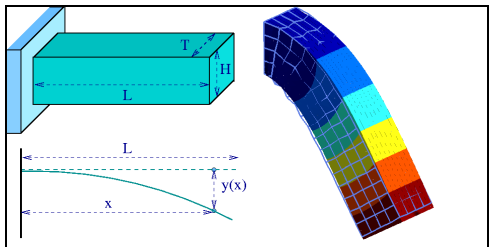

4x1x1 sampling: M=16.31%, SD=2.83%, MAX=38%
8x2x2 sampling: M=7.08%, SD=0.58%, MAX=16.7%
16x4x4 sampling: M=0.68%, SD=0.03%, MAX=4.05%

Figure 6: (left) Cantilever submitted to gravity, (right) FEM reference solution with superposition of our 16x4x4 model, (see Fig 5 notations).

We notice that results are dependent of the sampling resolution, as for any other numerical method; however the fibber axis profile keeps close to the expected analytical.

6 CONCLUSIONS AND FUTURE WORK

We proposed a mass-spring model that ensures fast and physically accurate simulation of linear elastic, isotropic and homogeneous material. It consists in meshing any object by a set of cubic mass-spring elements, and in adding some corrective forces orthogonal to elongation forces. By construction, our model is well characterised by the Young's modulus, Poisson's ratio, shearing modulus and bulk modulus, for small deformations. The spring coefficients have just to be initialized according to simple analytic expressions. The amplitude of the corrective forces is simply derived from the elongation forces. Limits of our model have been given by comparing our results with those obtained by a

finite element method, chosen as reference for preciseness. We exhibited that our model can also support large deformations. The accuracy increases with the mesh resolution.

In the future, we are looking to apply the same technique to other geometrical elements, for example parallelepipeds, tetrahedron or any polyhedron. This would increase the geometrical reconstruction possibilities and would offer more tools for simulating complex shapes.

Mesh optimization or local mesh adaptation would probably improve the efficiency of the model. For example, we can modify the resolution in the vicinity of highly deformed zones, reducing large rotations of elements undergoing heavy load.

Moreover, it may be interesting to investigate a procedure to update the spring coefficients and corrective forces when the deformations become too large.

BIBLIOGRAPHY

[1] Baudet V., Beuve M., Jaillet F., Shariat B., Zara F.: *A New Mass-Spring System Integrating Elasticity Parameters in 2D.* RR-LIRIS-2007-003, LIRIS UMR 5205 CNRS/ Univ. Lyon 1, February 2007.

[2] Bianchi G., Solenthaler B., Székely G., Harders M.: *Simultaneous topology and stiffness identification for mass-spring models based on FEM reference deformations.* In MICCAI 2004 (Berlin, 2004), Springer-Verlag, (Ed.), pp. 293–301.

[3] Cotin S., Delingette H., Ayache N.: *Efficient linear elastic models of soft tissues for real-time surgery simulation.* Proceedings of the Medecine Meets Virtual Reality (MMVR 7) 62 (1999), 100–101.

[4] Deussen O., Kobbelt L., Tucke P.: *Using simulated annealing to obtain good nodal approximations of deformable objects.* In Proceedings of the 6th Eurographics Workshop on Animation and Simulation (Berlin, 1995), Springer-Verlag, pp. 30–43.

[5] Nealen A., Müller M., Keiser R., Boxerman E., Carlson M.: *Physically based deformable model in computer graphics.* Eurographics (2005). State of the Art report.

[6] Picinbono G., Delingette H., Ayache N.: *Non-linear anisotropic elasticity for real-time surgery simulation.* Graphical Model (2003).

[7] Van Gelder A.: *Approximate simulation of elastic membranes by triangulated spring meshes.* Journal of Graphics Tools 3, 2 (1998), 21–42.